

Vibration-based damage detection in wind turbine towers using artificial neural networks

Cong-Uy Nguyen^a, Thanh-Canh Huynh^b and Jeong-Tae Kim^{*}

*Department of Ocean Engineering, Pukyong National University,
599-1 Daeyon-3dong, Nam-gu, Busan 608-737, Republic of Korea*

(Received November 11, 2018, Revised November 25, 2018, Accepted November 28, 2018)

Abstract. In this paper, damage assessment in wind-turbine towers using vibration-based artificial neural networks (ANNs) is numerically investigated. At first, a vibration-based ANNs algorithm is designed for damage detection in a wind turbine tower. The ANNs architecture consists of an input, an output, and hidden layers. Modal parameters of the wind turbine tower such as mode shapes and frequencies are utilized as the input and the output layer composes of element stiffness indices. Next, the finite element model of a real wind-turbine tower is established as the test structure. The natural frequencies and mode shapes of the test structure are computed under various damage cases of single and multiple damages to generate training patterns. Finally, the ANNs are trained using the generated training patterns and employed to detect damaged elements and severities in the test structure.

Keywords: wind turbine; vibration; frequency; mode shape; ANN; damage detection; finite element model

1. Introduction

Wind energy is a promising alternative source in the world's future because it produces no greenhouse gas, which is the main cause of global warming. Following the global trend, Korea has concentrated to develop small- and medium-sized wind farms. Especially Jeju Island has an ambitious plan to be a Carbon Free Island by 2030 (Park 2015). In order to fulfill the clean energy demand, more wind turbine towers will be installed in the coming years. The strong investment into wind energy harvest leads to the consideration of safety and durability of the wind turbine tower (WTT). During the lifetime, the slender vertical wind tower exposes to extreme wind frequently, so it experiences large deflections and repeated stress cycles, which would cause damage in the WTT (Benedetti *et al.* 2011, Park *et al.* 2015).

Structural health monitoring based on modal properties can be a solution to ensure the safety as well as the serviceability of the WTT (Li *et al.* 2014, Kim *et al.* 2014, Nguyen *et al.* 2015, Martinez-Luengo *et al.* 2016, Nguyen *et al.* 2017). It is well-proven that structural damage causes

*Corresponding author, Professor, E-mail: idis@pknu.ac.kr

^a Graduate Student, E-mail: uyznob@gmail.com

^b Postdoctoral Researcher, E-mail: ce.huynh@gmail.com

the change of mechanical parameters such as mass and stiffness. Consequently, it alters the dynamic characteristics of the system including modal parameters (Pandey *et al.* 1994). In the past, there were considerable efforts in vibration-based structural health monitoring which utilized dynamic measurement to extract damage sensitive features. Many researchers employed the change in natural frequencies and mode shapes for damage detection and structural identification (Vandiver 1977, Farrar *et al.* 1994, Kim *et al.* 1995, Kim *et al.* 2003, Huynh *et al.* 2016, Li *et al.* 2016). Nguyen *et al.* (2015) investigated the potential of the frequency-based and mode shape-based methods for health monitoring of a numerical WTT model. They later used the frequency-based method to detect damaged joints in a lab-scaled WTT (Nguyen *et al.* 2017). From their findings, it is shown that the high stiffness of the segmental joints in the WTT could cause discontinuities in mode shapes and modal curvatures that may result in inaccurate damage localization. Thus, an alternative method should be sought.

Along with various damage detection methods, the artificial neural network (ANN) has an excellent performance in damage pattern recognition (Yun *et al.* 2004, Park *et al.* 2009), which has been widely applied as the damage identification aid. Auto-associative neural networks were developed to monitor the cable-stayed Kap Shui Mun bridge (Hong Kong) via measured modal data from an online system (Ni *et al.* 2002). Li *et al.* (2007) identified damage in a beam via ANN based on statistical properties of structural dynamic response. Transverse crack in a beam was investigated via developing a neural network in which the input parameters were first three natural frequencies and the output parameter were relative crack depth and relative crack location in dimensionless forms (Sutar *et al.* 2015). Shu *et al.* (2012) employed changes of variances and covariance of structural dynamic responses for training ANN to localize damage in railway bridge under train-induced vibrations.

Despite those research efforts, the implementation of the ANNs to damage identification in the WTT has not studied so far. A well-established and sufficiently trained ANNs model could be an important component in the real-time health monitoring system of the WTT. This current study focuses on the possibility of employing the vibration-based ANNs for the identification of damage location and severity in the WTT. The remaining is arranged as follows. Firstly, a vibration-based ANNs algorithm is established for single and multiple structural damages in the WTT. The modal parameters including normalized natural frequencies and mode shapes are selected as the input, while the output layer is composed of element stiffness indices. Next, the finite element model of a real WTT is established as the test structure. Natural frequencies and mode shapes of the test structure are extracted from the modal analysis under a number of damage cases. Finally, the ANNs are trained using the training patterns generated from those damage cases. The trained ANNs are then employed to detect damaged elements and their severities for the test structure.

2. Vibration-based damage detection method using artificial neural networks

2.1 Schematic of damage detection method

The vibration-based damage detection method using ANNs is schematized in Fig. 1. The algorithm used feed-forward neural networks wherein connections between the units do not form a cycle. The ANNs architecture consists of an input, an output, and hidden layers. The activation functions are sigmoid in the hidden layers and linear function in the output layer. The scheme of the method includes two parts: (a) Training modal properties-based ANNs and (b) Damage

detection for the WTT using the trained ANNs.

The training of modal properties-based ANNs is performed in the following five steps: (1) a baseline finite element model of a WTT is established from structural analysis by ANSYS S/W. This FE model is coded via ANSYS Parametric Design Language (APDL) in order to auto-analyze a large number of damage scenarios. (2) single and multiple damage scenarios are selected on the basis of the potential damage in the WTT. Each damage scenario contains two important parameters which are location and severity. The single damage can locate at any segments of the FE model while the multiple damages are assumed only at 4 connection flanges to reduce the computational cost. (3) the modal analysis of the WTT model with every damage scenario is proceeded. (4) modal parameters (i.e., mode shapes and natural frequencies) are acquired using modal identification methods such as frequency domain decomposition, or stochastic subspace identification (Yi and Yun 2004, Qu *et al.* 2017) and saved into a database for single and multiple damages detections, independently. (5) these data sets are later used for training modal parameters-based ANNs. Four ANNs are built for single and multiple damage detection of the WTT. They are frequency-based ANNs for single damage detection (FAS), frequency-based ANNs for multiple damage detection (FAM), mode shape-based ANNs for single damage detection (MAS), mode shape-based ANNs for multiple damage detection (MAM).

The damage detection for the WTT is performed as follows: first, acceleration signals from sensors on the WTT are recorded during operation; second, the modal parameters are extracted and classified as natural frequencies and mode shapes separately; and third, the WTT status can be monitored via the FAS and the MAS for single damage detection. Simultaneously, the flange connections are checked up via the FAM and the MAM for multiple damage detection.

The output of the FAS and MAS are the damage severity of each element in the WTT model as defined in Eq. (2). Meanwhile, the FAM and MAM provide damage severities of all four flange connections. The damage severity is introduced as the reduction of element stiffness k . The element stiffness S_i index is defined as

$$S_i = k_{i,d}/k_{i,u} \tag{1}$$

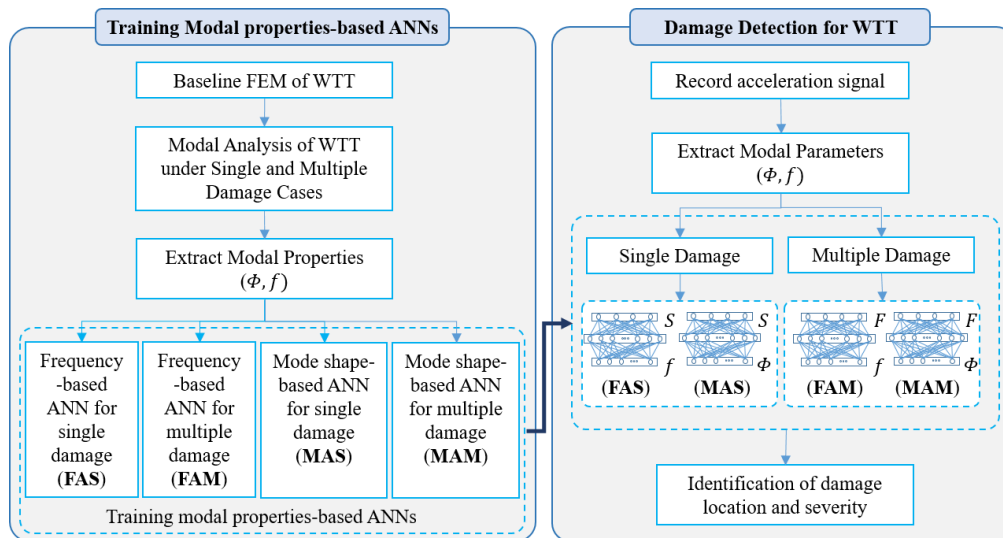


Fig. 1 Scheme of vibration-based damage detection method using ANNs

where i denotes element number; d and u denotes damaged and intact case. Besides, the segment damage severity is defined as

$$\alpha = 1 - S_i \quad (2)$$

2.2 Frequency-based ANNs

The frequency-based ANNs algorithms (i.e., FAS and FAM) for damage detection are designed with feed-forward neural networks. The input layer is composed of natural frequencies of the WTT. For better training results, the normalized natural frequencies from first three modes along the wind direction (X direction) and cross-wind direction (Y direction) are selected as the input of frequency-based ANN, which is described in Eq. (3).

$$f = [f_{x1} \ f_{x2} \ f_{x3} \ f_{y1} \ f_{y2} \ f_{y3}] \quad (3)$$

The normalization of natural frequencies is defined as in Eq. (4).

$$\|f_0\|_2 = f_0^T f_0 = 1; \quad \|f_d\|_2 = f_d^T f_d = 1 \quad (4)$$

where subscripts 0 and d denote the intact and damaged cases, respectively. In single damage detection for the WTT, only one segment is randomly damaged with the severity ranging from 5% to 50% with a step of 5%. Totally, there are 71 cylinder segments can be damaged in the tower. Therefore, the FAS for single damage detection is trained with 710 patterns. Meanwhile, the multiple damage detection only considers flange connections as potential locations. It is noted that they are the most vulnerable parts of the WTT during operation. Because the multiple damages with random severity ranging from 0% to 45% with a step of 5% can appear at any of four flange connections, there are 10000 training patterns for the FAM. The number of hidden layers and neurons in each layer for the FAS and FAM are summarized as in Table 1.

As shown in Fig. 2, the FAS has 6 neurons for normalized natural frequencies in the input layer and 71 neurons for the segmental damage severity in the output layer. There are 2 hidden layers in the FAS. The first hidden layer is composed of 35 neurons, while the second one is composed of 71 neurons. Fig. 3 shows that the FAM has 6 neurons for normalized natural frequencies in the input layer and 4 neurons for the flange damage severity in the output layer. The hidden layer of FAM is composed of 50 neurons. After a sufficient training, the frequency-based ANNs including FAS and FAM are employed to identify damage with severity staying out the training values.

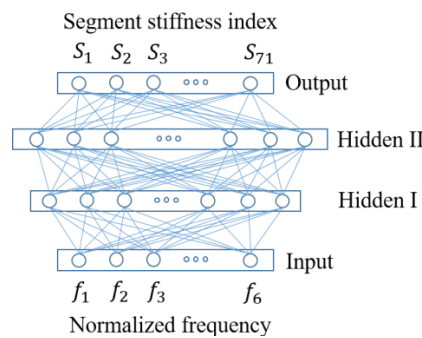


Fig. 2 The FAS architecture

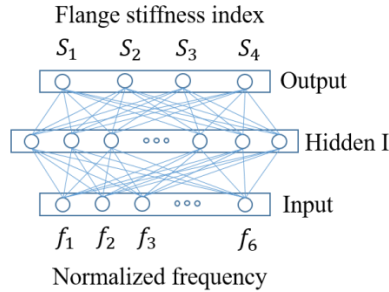


Fig. 3 The FAM architecture

Table 1 Properties of frequency-based ANNs for damage detection

ANN Properties	FAS	FAM
No. Training Patterns	710	10000
No. Input Neurons	6	6
No. Hidden 1 Neurons	35	50
No. Hidden 2 Neurons	71	-
No. Output Neurons	71	4

2.3 Mode shape-based ANNs

The mode shape-based ANNs algorithms (i.e., MAS and MAM) for damage detection are designed with feed-forward neural networks. The input layer is composed of mode shapes of the WTT. For better training results, the normalized mode shapes from the first three modes in the along-wind direction are selected as the input of mode shape-based ANN, which is described in Eq. (5).

$$\phi = [\phi_{x1} \ \phi_{x2} \ \phi_{x3}] \tag{5}$$

where the ϕ_{xi} is the eigenvector of the i^{th} mode in the along-wind direction. Near the support of WTT, the displacement around zero are excluded from the input vector.

The normalization of mode shapes are defined as in Eq. (6).

$$\|\phi_0\|_2 = \phi_0^T \phi_0 = 1; \ \|\phi_d\|_2 = \phi_d^T \phi_d = 1 \tag{6}$$

where subscripts 0 and d denote the intact and damaged cases, respectively. In single damage detection for the WTT, only one segment is randomly damaged with the severity ranging from 5% to 50% with a step of 5%. Similar to the FAS, the MAS for single damage detection is trained with 710 patterns. Meanwhile, the multiple damage detection only considers flange connections as potential inflicted locations. Because the damage with random severity ranging from 0% to 45% with a step of 5% can appear at four flange connections, the MAM is trained with 10000 patterns as in the FAM. The number of hidden layers and neurons in each layer for the MAS and MAM are summarized as in Table 2.

Table 2 Properties of mode shape-based ANNs for damage detection

ANN Properties	MAS	MAM
No. Training Patterns	710	10000
No. Input Neurons	203	203
No. Hidden 1 Neurons	69	50
No. Hidden 2 Neurons	71	4

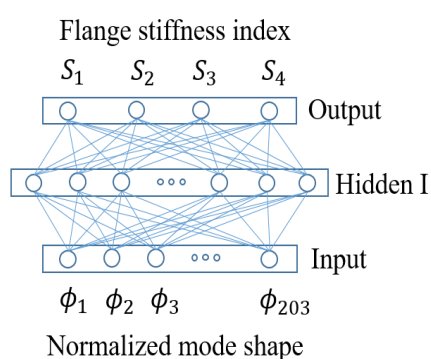


Fig. 4 The MAS architecture

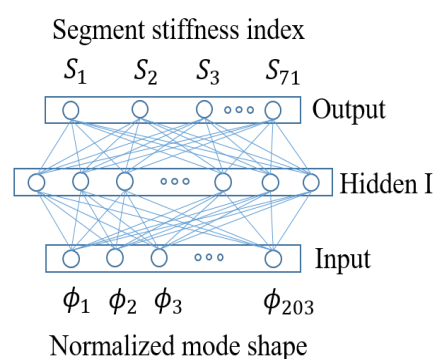


Fig. 5 The MAM architecture

As presented in Fig. 4, the MAS has 203 neurons for normalized mode shapes in the input layer and 71 neurons for the segmental damage severity in the output layer. Meanwhile, the hidden layer is composed of 69 neurons. Besides, Fig. 5 shows that the MAM has 203 neurons for normalized mode shapes in the input layer and 4 neurons for the flange damage severity in the output layer. The hidden layer of FAM is composed of 50 neurons. After sufficient training, the frequency-based ANNs including MAS and MAM are employed to identify damage with severity staying out the training values.

3. Finite element modeling of wnd turbine tower

The finite element model of a real WTT structure is established as the test model. The real WTT is located in the Hankyung II Wind Park, Jeju Island, Korea. The type of the WTT is V90-3.0 MW with nominal rating 3000 kW. The cut-in wind speed is 4 m/s while the cut-out and 25 m/s. There are 3 blades up-wind direction. Nacelle and Rotor weigh 68 and 39.8 ton, respectively. The real structure is 80 m high including the hub. There are 4 main segments in the tower. Each main segment has a flange at 2 tips so each one can combine together through bolt connections. The first segment is embedded in the foundation and the only 0.55 m is above the foundation surface. The second segment is 19.21m long while two remaining segments are around 29 m. Each main segment is formed by several sections with the thickness changing along elevation. Table 3 lists the variation of the section's thickness with respect to the increasing height. The tubular tower material is S355 J2G31. The top-level diameter is 2.316 m and the bottom level is 4.150 m.

As shown in Fig. 6, the finite element WTT model is simulated in ANSYS. The rotor and nacelle are simulated as lump masses on the top of the tower in the right dimension. These masses are linked rigidly to the top flange of the WTT. In order to generate a database of modal parameters in each damage scenario, the finite element model is divided into 71 cylinder segments.

Each cylinder segment is composed of 36 shell elements along the perimeter. The height of each element depends on the diameter of each segments ranging from 1.8 m in the bottom to 1 m in the top. The modal analysis of the intact WTT shows the first three mode shapes along-wind direction and cross-wind direction, as in Fig. 7. The rotor and nacelle axis is always perpendicular with flange 4 in every mode. This confirms the assumption of rigid links between those elements.

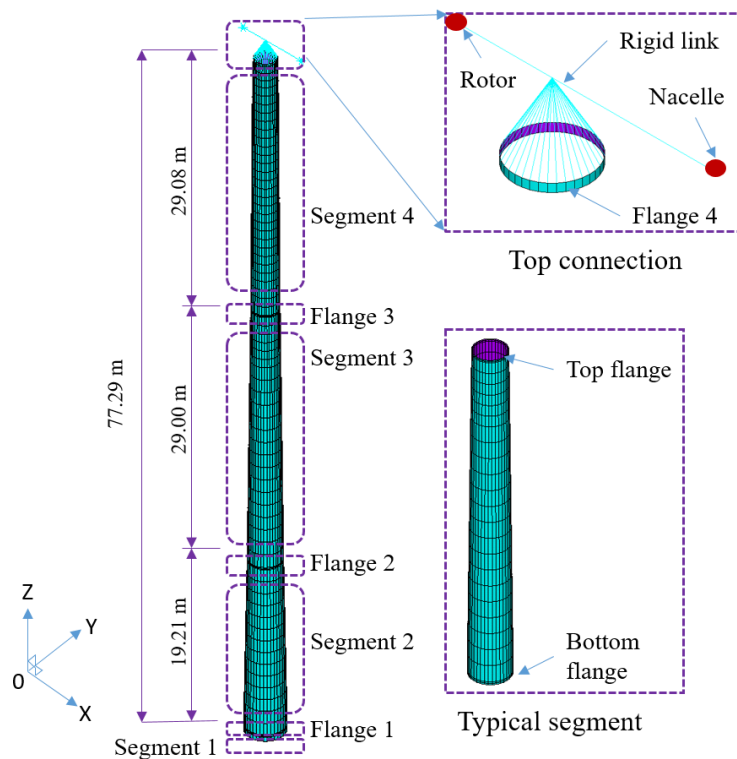


Fig. 6 Finite element modeling of the WTT

Table 3 Cross-sectional thickness of the WTT model

Height (m)	0 ÷ 5.4	5.4 ÷ 21.9	21.9 ÷ 30.6	30.6 ÷ 36.4	36.4 ÷ 42.2	42.2 ÷ 50.9	50.9 ÷ 53.8	53.8 ÷ 56.7	56.7 ÷ 59.6	59.6 ÷ 77.3
Thickness (mm)	40	26	24	23	22	21	19	18	17	16

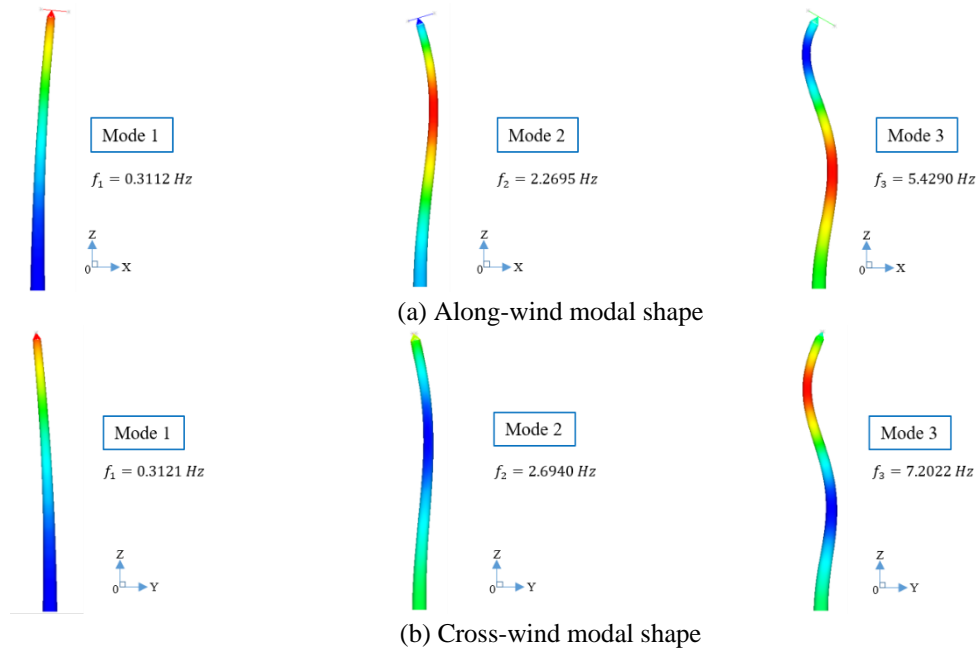


Fig. 7 Modal analysis results for the WTT model

4. Damage detection in wind turbine tower using vibration-based ANNs

4.1 Detection of single damage

Damage detection via FAS

Six test cases are selected to demonstrate the performance of single damage detection via the trained FAS, as listed in Table 4. The infliction is located randomly from the bottom to the top of the WTT model with severity ranging from 12% to 18%. The first three cases (Cases 1-3) are trained patterns, while the 3 remaining cases (Cases 4-6) are untrained patterns. The damage location and severity predicted via the FAS are presented in Fig. 8. As shown in the figure, the damage locations are recognized correctly via the FAS. However, the estimated damage severities are below the inflicted ones.

Damage detection via MAS

Six test cases are selected to demonstrate the performance of single damage detection via the MAS, as listed in Table 5. The infliction is located randomly from the bottom to the top of the WTT model with severity ranging from 10% to 25%. The first three cases (Cases 1-3) are trained patterns, while the 3 remaining cases (Cases 4-6) are untrained patterns. The damage location and severity predicted via the MAS are shown in Fig. 9. It is observed that the damage locations are recognized correctly via the MAS. However, the estimated damage severities are below the inflicted ones.

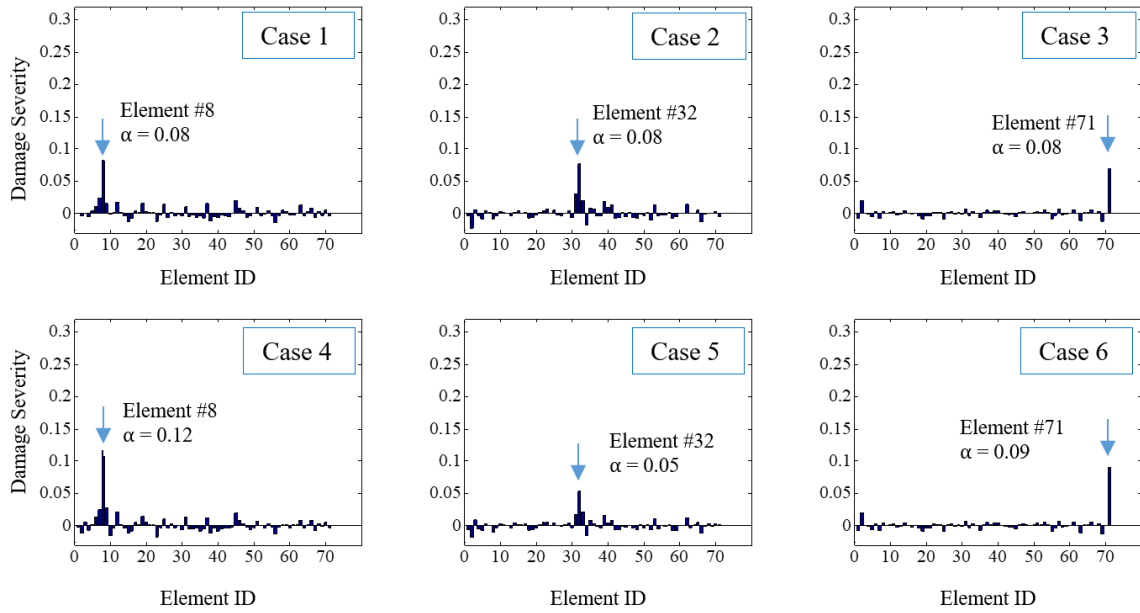


Fig. 8 Damage detection in the WTT model via the FAS

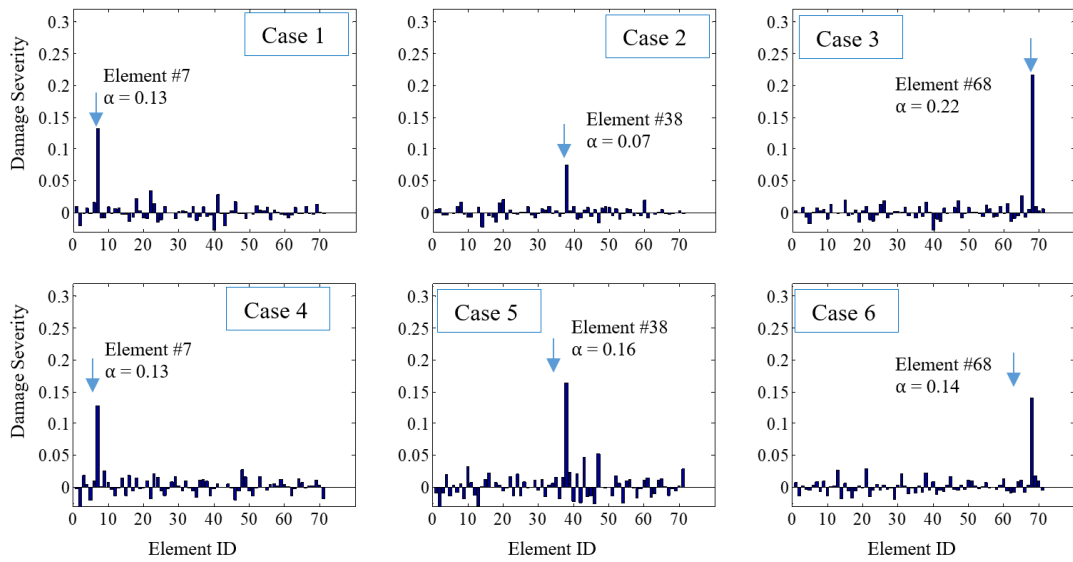


Fig. 9 Detection results for single damage in the WTT via the MAS

Table 4 Test cases for the FAS

Damaged Element	Trained Patterns			Untrained Patterns		
	Case 1	Case 2	Case 3	Case 4	Case 5	Case 6
ID	8	32	71	8	32	71
Severity	15%	15%	15%	18%	12%	16%

Table 5 Test cases for the MAS

Damaged Element	Trained Patterns			Untrained Patterns		
	Case 1	Case 2	Case 3	Case 4	Case 5	Case 6
ID	7	38	68	7	38	68
Severity	15%	10%	25%	18%	24%	18%

4.2 Detection of multiple damage

Damage detection via FAM

Six test cases are selected to demonstrate the performance of multiple damage detection via the FAM, as shown in Table 6. The infliction is located randomly in any of the four flange connections with severity ranging from 5% to 45%. The first three cases (Cases 1-3) are trained patterns, while the 3 remaining cases (Cases 4-6) are untrained patterns. The damage location and severity estimated by the FAM are presented in Fig. 10. As shown in the figure, the damage locations and severity are recognized correctly via the FAM.

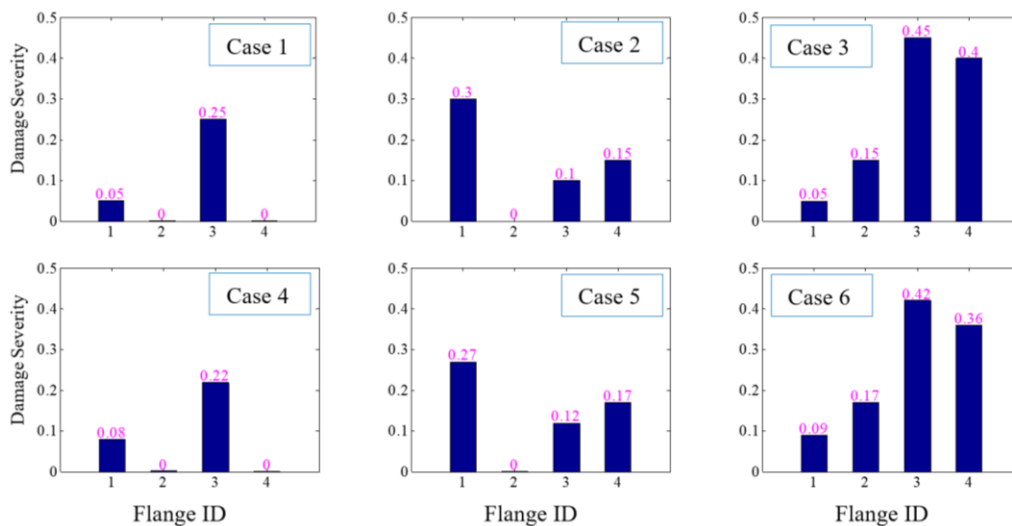


Fig. 10 Damage detection in the WTT via the FAM

Table 6 Test cases for the FAM

Damaged Flanges	Trained Patterns			Untrained Patterns		
	Case 1	Case 2	Case 3	Case 4	Case 5	Case 6
1	5%	30%	5%	8%	27%	9%
2	-	-	15%	-	-	17%
3	25%	10%	45%	22%	12%	42%
4	-	15%	40%	-	17%	36%

Damage detection via MAM

Six test cases are selected to demonstrate the performance of multiple damage detection via the MAM, as shown in Table 7. The infliction is located randomly in any of the four flange connections with severity ranging from 5% to 42%. The first three cases (Cases 1-3) are trained patterns, while the 3 remaining cases (Cases 4-6) are untrained patterns. The damage location and severity estimated by the MAM are presented in Fig. 11. As shown in the figure, the damage locations are recognized correctly, meanwhile, the damage severities are estimated around true values via the MAM.

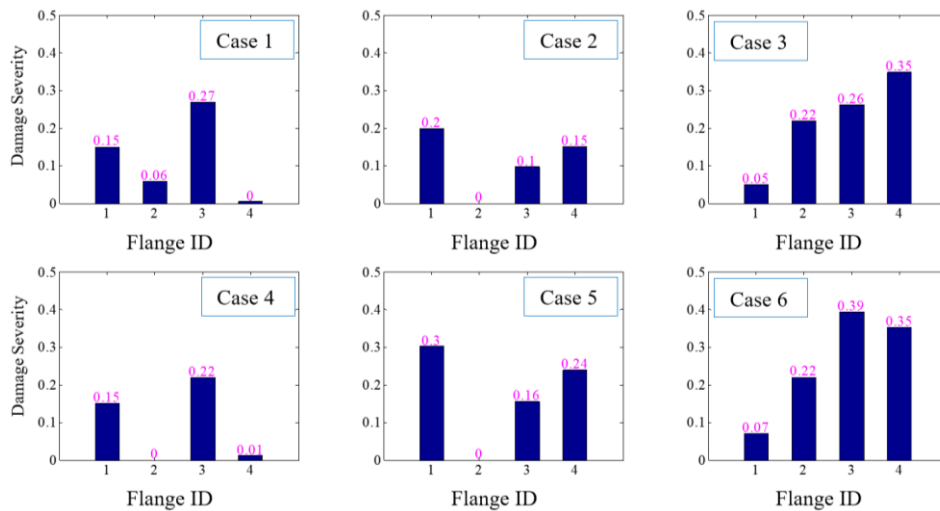


Fig. 11 Damage detection in the WTT via the MAM

Table 7 Test cases for the MAM

Damaged Flanges	Trained Patterns			Untrained Patterns		
	Case 1	Case 2	Case 3	Case 4	Case 5	Case 6
1	15%	20%	5%	8%	27%	9%
2	-	-	15%	-	-	17%
3	25%	10%	25%	22%	12%	42%
4	-	15%	35%	-	17%	36%

5. Conclusions

In this study, damage detection of a wind turbine tower (WTT) model using vibration-based artificial neural networks (ANNs) was presented. At first, a vibration-based ANNs algorithm was designed for damage detection in the WTT model. The ANNs architecture consisted of an input, an output, and hidden layers. Modal parameters of the wind turbine tower such as mode shapes and frequencies were utilized as the input and the output layer composes of element stiffness indices. Next, the finite element model of a real wind-turbine tower was established as the test structure. The natural frequencies and mode shapes of the test structure were computed under various damage cases to generate training patterns. Finally, the ANNs were trained using the generated training patterns and employed to detect damaged elements and severities in the test model.

The first three natural frequencies in the along-wind and cross-wind directions were employed for the frequency-based ANNs. Meanwhile, only the first three mode shapes in the along-wind were employed for the mode shape-based ANNs. The structural damages were introduced as the reduction of element stiffness in the WTT. In case of single damage, the infliction was simulated randomly at any segment in total 71 locations; whereas multiple damages only located at 4 flange connections. The designed vibration-based ANNs were successful in indicating single-damage as well as multi-damage locations in the WTT structure. However, the structural damage severity was only identified correctly via the frequency-based method while the remaining ANNs estimated infliction severity around the true values for all cases. It is noted that the frequency-based ANNs were quite better than mode shape-based ANNs in damage location and severity estimation. Future studies remain to evaluate the accuracy of the FE model by comparing with the experimental result, and to detect damage below 5% severity in the WTT.

Acknowledgements

This work was supported by a Research Grant of Pukyong National University (2017 year).

References

- Benedetti, M., Fontanari, V. and Zonta, D. (2011), "Structural health monitoring of wind towers: remote damage detection using strain sensors", *Smart Mater. Struct.*, **20**, 1-13.
- Farrar, C.R. (1997), "System identification from ambient vibration measurements on a bridge", *J. Sound Vib.*, **205**(1), 1-18
- Huynh, T.C., Park, J.H. and Kim, J.T. (2016), "Structural identification of cable-stayed bridge under back-to-back typhoons by wireless vibration monitoring", *Measurement*, **88**, 385-401.
- Kim, J.T. and Stubbs, N. (1995), "Model uncertainty and damage detection accuracy in plate-girder bridges", *J. Struct. Eng.*, **121**(10), 1409-1417
- Kim, J.T., Huynh, T.C. and Lee, S.Y. (2014), "Wireless structural health monitoring of stay cables under two consecutive typhoons", *Struct. Monit. Maint.*, **1**(1), 47-67.
- Kim, J.T., Ryu, Y.S., Cho H.M. and Stubbs, N. (2003), "Damage identification in beam-type structures: Frequency-based method vs mode-shape-based method", *Eng. Struct.*, **25**, 57-67.
- Lee, J.J., Lee, J.W., Yia, J.H, Yun, C.B. and Jung, H.Y. (2004), "Neural networks-based damage detection for bridges considering errors in baseline finite element models", *J. Sound Vib.*, **280**, 555-578
- Li, H.N., Li, D.S., Ren, L., Yi, T.H., Jia, Z.G. and LI, K.P. (2016), "Structural health monitoring of innovative civil engineering structures in Mainland China", *Struct. Monit. Maint.*, **3**(1), 1-32.

- Li, H.N., Yi, T.H., Ren, L., Li, D.S. and Huo, L.S. (2014), "Review on innovations and applications in structural health monitoring for infrastructures", *Struct. Monit. Maint.*, **1**(1), 1-45.
- Li, Z.X. and Yang, X.M. (2008), "Damage identification for beams using ANN based on statistical property of structural response", *Comput. Struct.*, **86**(1), 64-71.
- Martinez-Luengo, M., Lolios, A. and Wang, L. (2016), "Structural health monitoring of offshore wind turbines: A review through the statistical pattern recognition paradigm", *Renew. Sust. Energ. Rev.*, **64**, 91-105.
- Nguyen, C.U., Huynh, T.C., Dang, N.L. and Kim, J.T. (2017), "Vibration-based damage alarming criteria for wind turbine towers", *Struct. Monit. Maint.*, **4**(3), 221-236.
- Nguyen, T.C., Huynh, T.C. and Kim, J.T. (2015), "Numerical evaluation for vibration-based damage detection in wind turbine tower structure", *Wind Struct.*, **21**(6), 657-675.
- Nguyen, T.C., Huynh, T.C., Yi, J.H. and Kim, J.T. (2017), "Hybrid bolt-loosening detection in wind turbine tower structures by vibration and impedance responses", *Wind Struct.*, **24**(4), 385-403.
- Ni, Y.Q., Zhou, X.T., Ko, J.M. and Wang, B.S. (2002), "Vibration-based damage localization in Ting Kau Bridge using probabilistic neural network", *Adv. Struct. Dynamics*, **2**, 1069-1076.
- Pandey, A.K. and Biswas, M. (1994), "Damage detection in structures using changes in flexibility", *J. Sound Vib.*, **169**(1), 3-17.
- Park, J. (2015), Annual Report on Wind Energy Industry of Korea 2015, *Korea Wind Energy Industry Association*
- Park, J.H., Huynh, T.C., Choi, S.H. and Kim, J.T. (2015), "Vision-based technique for bolt-loosening detection in wind turbine tower", *Wind Struct.*, **21**(6), 709-726.
- Park, J.H., Kim, J.T., Hong, D.S., Ho, D.D. and Yi, J.H. (2009), "Sequential damage detection approaches for beams using time-modal features and artificial neural networks", *J. Sound Vib.*, **323**(1-2), 451-474.
- Qu, C.X., Yi, T.H., Yang, X.M. and Li, H.N. (2017), "Spurious mode distinguish by eigensystem realization algorithm with improved stabilization diagram", *Struct. Eng. Mech.*, **63**(6), 743-750.
- Shu, J., Zhang, Z., Gonzalez, I. and Karoumi, R. (2012), "The application of a damage detection method using Artificial Neural Network and train-induced vibrations on a simplified railway bridge model", *Eng. Struct.*, **52**, 408-421.
- Sutar, M.K., Sarojrani, P. and Jayadev, R. (2015), "Neural based controller for smart detection of crack in cracked cantilever beam", *Proceeding of Materials Today*, **2**, 2648-2653.
- Vandiver, J.K. (1977), "Detection of structural failure on fixed platforms by measurement of dynamic response", *J. Petrol. Technol.*, **29**(3), 305-310.
- Yi, J.H. and Yun, C.B. (2004), "Comparative study on modal identification methods using output-only information", *Struct. Eng. Mech.*, **17**(3-4), 445-466.